PROCEEDINGS OF SCIENCE

Digital FDIRC: a Focused Differential Internal Reflection Cherenkov imaged by SiPM arrays

P.S. Marrocchesi[ab*], **M.G. Bagliesi**[ab], **A. Basti**[bc], **G. Bigongiari**[ab], **S. Bonechi**[ab], **P. Brogi**[ab], **C. Checchia**[d], **G. Collazuol**[d], **P. Maestro**[ab], **F. Morsani**[ab], **C. Piemonte**[e], **F. Stolzi**[ab], **J.E Suh**[ab], **A. Sulaj**[ab]

[a] *Dept.of Physical Sciences, Earth and Environment, Univ. of Siena, 53100 Siena, Italy*
[b] *INFN Sezione di Pisa, Largo Bruno Pontecorvo 3, 56127 Pisa, Italy*
[c] *Dept. of Physics, Univ. of Pisa, Largo Bruno Pontecorvo 3, 56127 Pisa, Italy*
[d] *Department of Physics and Astronomy, Univ. of Padova and INFN-Padova, 35131 Padova, Italy*
[e] *Fondazione Bruno Kessler (FBK), I-38122 Trento, Italy*
E-mail: marrocchesi@pi.infn.it

A prototype of an Internal Reflection Cherenkov, equipped with a SiO_2 (Fused Silica) radiator bar optically connected to a cylindrical mirror, was tested at CERN SPS in March 2015 with a beam of relativistic ions obtained from fragmentation of primary argon nuclei at energies 13, 19 and 30 GeV/n. The detector, designed to identify cosmic nuclei, features an imaging focal plane of dimensions $\sim$ 4 cm $\times$ 3 cm equipped with 16 arrays of NUV-SiPM (near-ultraviolet sensitive silicon photon avalanche detector) for a total of 1024 sensitive elements. The outstanding performance of the photodetectors (with negligible background in between adjacent photopeaks), allowed to apply the technique of photon counting to the Cherenkov light collected on the focal plane. Thanks to the fine granularity of the array elements, the Cherenkov pattern was recorded together with the total number of detected photoelectrons increasing as Z^2 as a function of the atomic number Z. In this paper, we report the performance of the SiPM arrays and the excellent resolution achieved by the Digital Cherenkov prototype in the charge identification of the elements present in the beam.

The 34th International Cosmic Ray Conference,
30 July- 6 August, 2015
The Hague, The Netherlands

*Corresponding author

PoS(ICRC2015)619

1. Introduction

The DIRC (Detection of Internally Reflected Cherenkov light) technique – whereby the Cherenkov light generated by the passage of a charged particle propagates via multiple internal reflections along a radiator bar of fused silica – was pioneered by the BaBar experiment at SLAC [1]. In the BaBar configuration, after reaching one end of the bar, the light crossed a standoff volume filled with water and was detected on a plane instrumented with an array of photomultipliers. The instrument was successfully operated as a particle identifier achieving a suitable ($> 3\sigma$) π-K mass separation for momenta up to 3 – 4 GeV/c.

The introduction of a focalization scheme (Focussing DIRC or FDIRC [2]) of the light emitted at one end of the radiator allows a drastic reduction of the so called "pinhole effect" [3] that causes a broadening of the Cherenkov image on the detection plane in proportion to the cross section of the radiator bar. The FDIRC concept has been applied to the experiment BELLE at KEK [4] and proposed as a particle identification detector for PANDA at FAIR [5] and in the SuperB design study [6]. In this paper, we report on the performance of an FDIRC prototype equipped with a cylindrical mirror implemented in a focussing block of fused silica (SiO_2). The Cherenkov light (Fig.1a) is focussed onto a mosaic of Silicon PhotoMultiplier (SiPM) arrays. High resolution imaging of the Cherenkov pattern is achieved on the focal plane thanks to the fine granularity of the photosensors.

The outstanding performance of the SiPM arrays allowed to operate the FDIRC prototype as a fully digital instrument and to use it as a photon counting device.

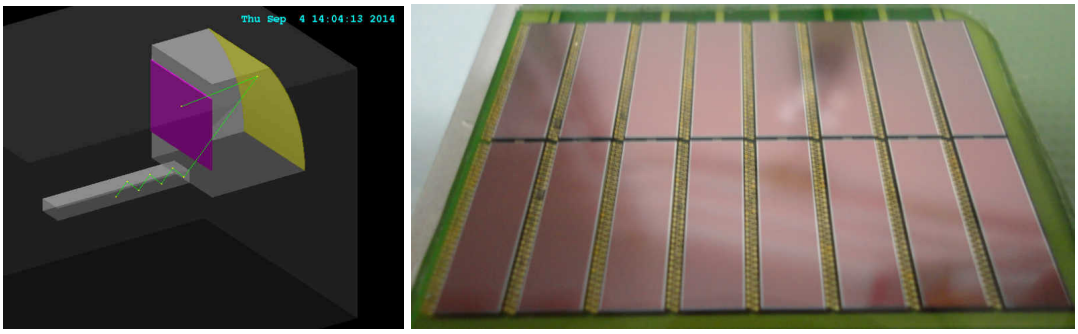

Figure 1: (a)Simulated optical propagation of a Cherenkov light-ray along the radiator bar in the FDIRC prototype as obtained with the GEANT4 ray-tracing package, (b) focal plane istrumented with a mosaic of 16 SiPM arrays for a total of 1024 SiPM photosensors.

2. Isotopic separation with an FDIRC

The construction of the prototype was motivated by a preliminary study [7] of the feasibility to achieve isotopic mass separation for cosmic nuclei by combining a velocity measurement with a precise determination of the particle momentum using an FDIRC in conjunction with a magnetic spectrometer. This possibility would open an interesting window for the measurements of the relative abundance of isotopes of cosmic origin and the energy dependence of their flux. In particular, some radioactive isotopes can provide valuable information on the confinement time of charged cosmic rays in the Galaxy. They can be regarded as cosmic *propagation clocks* as the knowledge of their decay time, together with a measurement of their relative abundance, can be used to test the predictions of cosmic-ray propagation models [8]. This is the case, for instance,

of the abundance ratio of the unstable ^{10}Be vs the stable ^{9}Be isotope, where the former decays with a mean lifetime of about 1.5×10^6 years. Measurements of the energy dependence of this ratio have been performed in space [9] and on balloons [10] but they are, at present, statistics limited above $\sim$ 1 GeV/n kinetic energy. At energies of a few 100 MeV/amu, detection techniques based on multiple dE/dx sampling, coupled with a measurement of the energy released in a thick absorber, have been used efficiently [9]. At higher energies, the Time of Flight (TOF) technique has been coupled with a rigidity measurement in the balloon experiment ISOMAX [10]. A window for Cherenkov detection opens above the threshold up to relativistic energies where the measurement of the velocity becomes impractical. In this energy domain, integral and/or differential measurements of Cherenkov light can be performed, using the Ring Cherenkov (RICH) or the FDIRC technique. A key factor to reach the required angular resolution and achieve a suitable mass discrimination for isotopes of astrophysical interest is the larger photostatistics provided by the Z^2 dependence of Cherenkov light emission for nuclei of charge Z with respect to particles with unit charge whereby the light yield is a limiting factor.

3. Construction of the FDIRC prototype

An FDIRC prototype was built by the Pisa/Siena group using a 20 cm long radiator bar of fused silica (SiO_2) shaped as a parallelepiped with 17.25 mm thickness, 35mm width and machined according to very severe specifications on the surface quality and geometry [11]. The bars were re-worked spare items from the former production of the $\sim$1.2 m long radiator bars of the BaBar experiment. In Fig.1a an example of the working principle of the detector is provided by a ray-tracing simulation by GEANT4 showing multiple reflections of a single Cherenkov photon along the bar, followed by a single reflection from the internal cylindrical surface of the mirror and final impact onto the focal plane. The measured dispersion curve for the refraction index n(λ) of the bar in [11] shows that for wavelengths larger than $\sim$350 nm, the index dependence on λ flattens and remains almost constant with a value n $\sim$1.47 in the spectral region covered by the SiPM. A focussing block of fused silica (Fig.1a) is optically connected to one end of the radiator bar and works by internal reflection as a cylindrical mirror with a radius of curvature of 26 cm. The mirror surface features an optical finish and Al coating. The lateral width of the focussing block is 14 cm and its height 16 cm. The lateral walls are not polished and have a diffusive surface texture. The reflectivity curve of the mirror is shown in Fig.2a. The focal plane is instrumented with a mosaic of 16 NUV-SiPM arrays for a total of 1024 SiPM sensors. Each array is finely segmented along the vertical direction into 64 SiPM units; the size of each SiPM is $\sim$4 mm x 0.2 mm and the gap between two adjacent SiPM units is 10 μm. The geometry of the array was designed to achieve a suitable vertical resolution for the reconstruction of the Cherenkov pattern. The arrays were developed by FBK (Trento) as p-over-n devices with NUV sensitivity [12, 13]. Each SiPM is comprised of 400 micro-cells of size 47.5 μm $\times$ 40 μm. Operated with an OverVoltage (OV) of 4.4 V, the measured Photon Detection Efficiency (PDE) of the SiPM is $\sim$35% at 420 nm and $\sim$27% at 360 nm, decreasing rapidly in the deeper UV where the index of refraction of fused silica has a strong chromatic dependence (Fig.2c). The effective spectral window for Cherenkov detection is therefore limited to an interval between 360 nm and 600 nm, a region where the index of refraction has a smooth wavelength dependence [11]. This design choice mitigates the otherwise important contribution of the chromatic error on the measurement of the Cherenkov angle. The price to pay is

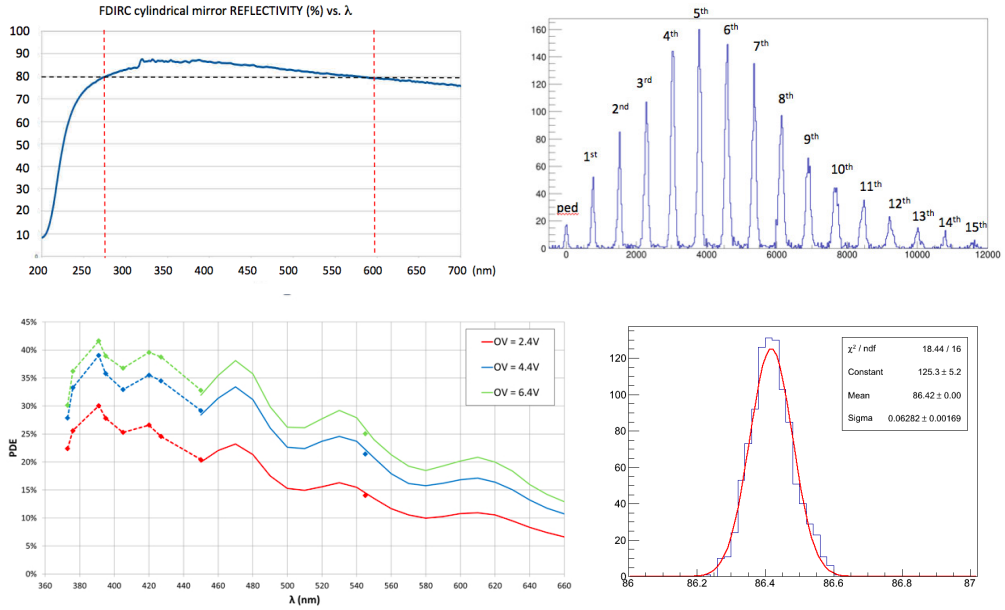

Figure 2: (a)(top-left) Internal reflectivity of the cylindrical mirror vs wavelength; (b)(top-right) photopeak spectrum from a single SiPM with Ar ions; (c)(bottom-left) Photon Detection Efficiency (PDE) as a function of wavelength, (d)(bottom-right) beam test data with Ar ions: distribution of the reconstructed vertical position of the apex of the hyperbola.

a reduction of the photon yield with respect to an instrument operating in a deeper UV regime. The SiPM arrays were micro-bonded to a multi-layered carrier-board to form a mosaic of 16 arrays as shown in Fig.1b. Given the large number of channels, high-density connectors were mounted on the back side of the carrier-board and the routing of the signals made use of 7 internal layers. The 1024 signals were then routed to the front-end board via 16 flat kapton cables, each carrying 64 signals. The SiPM arrays were fully characterized and showed a real breakthrough in the technology with a DCR lower than 100 kHz/mm^2 and almost negligible after-pulse rate ($< 5\%$) resulting in very well resolved photopeaks as shown, as an example, in Fig.2b where the spectrum from a single SiPM was obtained with a selection of Ar events.

4. Ion beam test at CERN in 2015

Although a test of the FDIRC isotopic mass separation performance should be planned with total particle momenta not larger than a few tens of GeV/c, in March 2015 we had the opportunity to perform a test at CERN with a beam of relativistic ions at 13, 19 and 30 GeV/amu. The velocity of the projectiles was too large for isotopic mass separation, nonetheless we could study the performance of the detector both in integral mode (charge separation of the beam fragments via an integral measurement of the Cherenkov light) and in differential mode (reconstruction of the Cherenkov angle). About 10 million triggers were recorded. The test took place at the SPS beamline H8 with a beam of relativistic ions obtained from fragmentation of primary argon nuclei onto an internal target of polyethylene and magnetically guided to the test area. Most of the data were taken with a beam setting that allowed only elements with A/Z=2 to reach the experimental area. This choice allowed the optimization of the elemental composition of the beam fragments for heavier nuclei up to Ar (to test the dynamic range of the detector). A drawback was the small

relative abundance of Be due to the absence of stable isotopes with the selected A/Z ratio. The beam test layout is sketched in Fig.3 where the FDIRC prototype was preceded by a pair of beam trigger scintillators in coincidence. A dedicated Beam Tracker (BT) – designed and built by our research group [14, 15] – was positioned along the beam line, downstream the FDIRC. An internal view of the prototype, enclosed in its light tight box, is shown in the same figure.

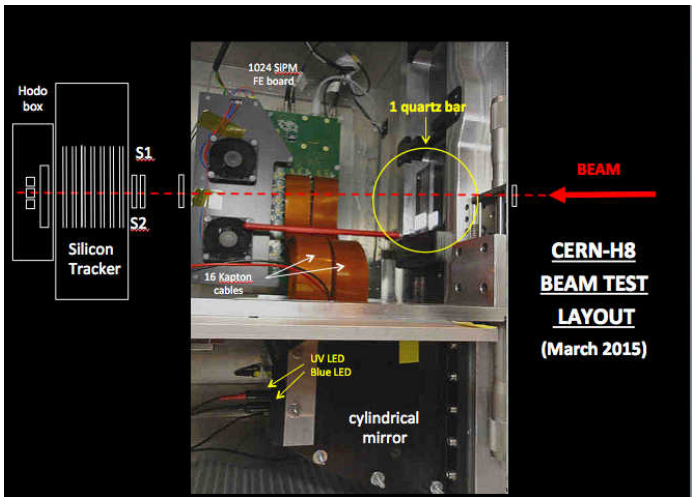

Figure 3: Beam test layout: internal view of the FDIRC inside its light-tight box. Beam particles impinge at normal incidence on a single radiator bar.

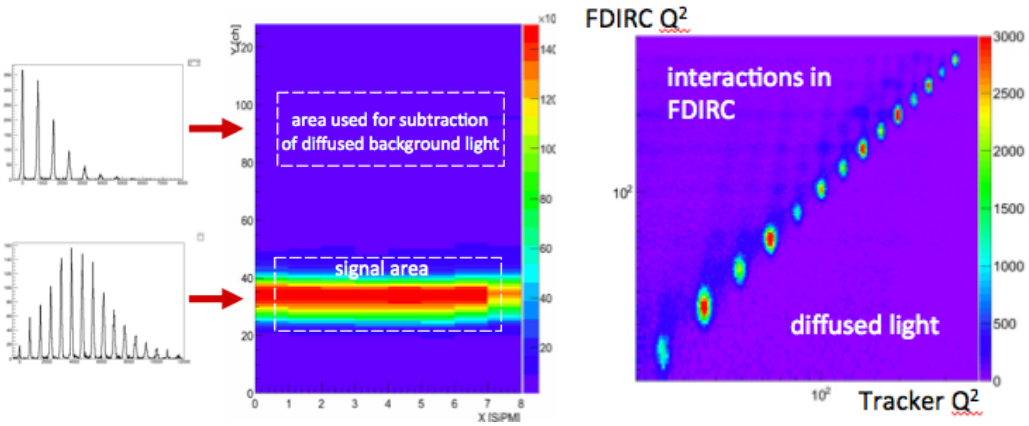

Figure 4: (a)(left) Example of SiPM spectra from the signal and background areas on the focal plane as defined in the text, (b) (right) Integral Cherenkov signal from FDIRC vs. the squared value of the charge measured by the Beam Tracker.

The Beam Tracker has two important roles: to reconstruct the incident beam track and to tag the particle's charge. It is subdivided into two sections: the Upper Tracker with a total of 4 layers of Si strip detectors and 4 layers of Si pixel arrays, followed by the Bottom Tracker with 3 double layers of Si strip detectors with strips alternately oriented along orthogonal directions. With respect to the 2013 beam test configuration – described in more detail in [16] – the BT configuration for the 2015 beam test was upgraded with the addition of two extra silicon strip detectors in the Bottom Tracker. With a maximum of 14 independent dE/dx measurements, the BT achieved a very accurate identification of the charge of the nucleus traversing the FDIRC, as shown in Fig.6a. This capability

turned out to be very effective to discriminate two classes of events: non-interacting beam particles and secondary products from the interaction of the incident particle in the FDIRC radiator.

5. Calibration and Data Analysis

Given the excellent separation of the photopeaks, the gain of each SiPM is easily estimated from the distance between the pedestal and the first photopeak and between two adjacent photopeaks. To reduce the uncertainty, the gain is calculated as an average over at least 4 intervals including the pedestal. The non uniformity of the gain over the whole focal plane turns out not to exceed 5%, inclusive of the contribution to the gain spread from the uncalibrated electronic readout channels. An important preliminary step in the analysis is to reject events where the incident ion has interacted in the radiator bar. This is made possible by a comparison between the charge measured by the Beam Tracker – positioned downstream the FDIRC – and the integral measurement of the Cherenkov light. A correlation plot is shown in Fig.4b where a simple diagonal cut is applied to select a clean sample of non-interacting events. After calibration, the signal from all SiPM channels inside the "signal area" illuminated by the Cherenkov pattern, and shown in Fig.4a, are summed up. An equivalent area, located far away from the signal region and shown in the same picture, is chosen as "background area" to provide a measurement of the diffused light background impinging on the focal plane. For each element selected by the BT, an estimate of the number N_{pe} of detected photoelectrons is obtained as the ratio of the integrated ADC counts from the signal region and the gain. After fitting the distribution with a gaussian, the mean value μ is plotted as a function of Z^2 in Fig.5a showing the expected quadratic dependence of the Cherenkov light yield on the atomic number for events taken with one radiator bar. Also shown in the same picture is the behavior of the diffused light integrated over the background region: it amounts to less than 5% of the signal and follows the same Z^2 dependence. This suggests that background light is a small fraction of the total Cherenkov light produced by the particle and it may originate from diffusion inside the focussing block (mainly from the lateral walls). The (Z independent) contribution from external light leaking inside the light-tight box is negligible. An additional background contribution is due to the SiPM dark count rate, which is present in both the signal and background reference areas and therefore almost completely eliminated by the background subtraction procedure. This contribution has been measured separately, using "random triggers" taken during the inter-spill phase of beam extraction. These pedestal events, recorded "off beam", are a very useful source of information to monitor the behavior of the detector and of the readout electronics as a function of time. The distribution of SiPM pedestals shows a fraction of spurious signals, mainly accumulating around the position of the first photopeak, that are due to the DCR. The cumulative number of DCR counts per event was found to be less than $\sim$10 over the whole instrumented focal plane. After subtraction of the diffuse light background contribution, the linear dependence with Z^2 of the Cherenkov integral signal is shown in Fig.5a for a single bar radiator. The same analysis is repeated for events taken with two radiator bars and shown in Fig.5b where the light yield is found to scale linearly with the radiator thickness, as expected. Due to the clear separation among adjacent photopeaks, the detector can be used in photon counting mode. Assuming that the fluctuations on the number of photoelectrons are dominated by the photostatistics of the Cherenkov light production, and in the limit of a purely Poissonian process, the Z dependence of the standard deviation σ is expected to be linear as shown in Fig. 5c. As the N_{pe} estimator is taken as representative of the charge of the beam particle, two

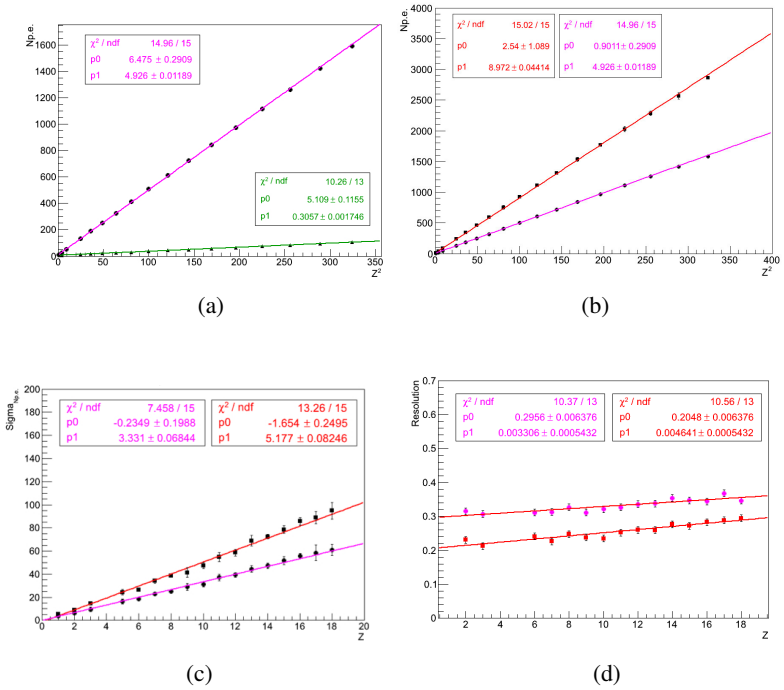

Figure 5: Integral Cherenkov signal from FDIRC vs. Z^2 with (a) one radiator bar in the signal region (upper curve) and in the background region (lower curve). With one and two radiator bars in the signal region: (b) Integral Cherenkov signal vs. Z^2 ; (c) sigma vs. Z; (d) charge separation vs. Z for ions differing by one unit of charge.

elements differing by one unit of charge can be resolved with a charge separation power defined as: $\frac{<\sigma>}{\mu(Z+1)-\mu(Z)}$ where the numerator is the average of the standard deviations for the two elements. This quantity is often referred to as "charge resolution" and expressed in units of the electron charge. It is expected to be independent of Z if the variance of the N_{pe} distribution is dominated by photostatistics. However, other sources of fluctuations, including noise from the photodetector and FE electronics, can contribute to an overall excess noise figure and be responsible for a deviation from a Z-independent resolution. This is visible in Fig.5d where a small residual Z dependence is observed for data taken with both one and two bars radiators.

The ability of the FDIRC to perform charge identification can be seen in Fig.6b where the integral signal from the prototype is computed from online data (i.e.: without offline calibrations and corrections) showing a well resolved charge spectrum of the beam fragments.

During the test, the nominal beam direction was at normal incidence on the radiator. Neglecting second-order effects due to the (small) beam divergence, the expected Cherenkov pattern on the focal plane (FC) is hyperbolic. In the local coordinate system of the FC, each SiPM can be treated as a "pixel" of dimensions $\sim$4 mm along the x-axis (horizontal) and 0.2 mm size along the y-axis (vertical). For each event, a threshold of 0.5 p.e. was first applied to all channels. Then, for all (n) SiPM in a vertical column corresponding to the x_i coordinate, a weighted average position $<y_i>$ was calculated as $< y_i >= \frac{\sum_{k=1}^{n} y_k p_k}{\sum_{k=1}^{n} p_k}$ where the nominal vertical position y_k of each SiPM was weighted with its digitized signal p_k. After repeating this procedure for all columns along the x-axis, the $<y_i>$ points with their respective errors σ_i were fitted with

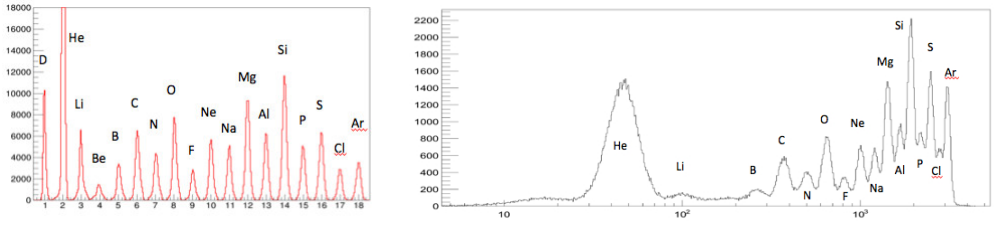

Figure 6: (a)(left) An example of the charge tagging provided by the Beam Tracker. Elements from Z=1 to Z=18 are clearly separated. The dominant He peak has been cut in the figure to show the less abundant elements, yet retaining a linear vertical scale (b)(right) Online plot of the integrated Cherenkov signal from the FDIRC prototype, representative of the charge spectrum of beam fragments (the horizontal log scale is units of number of photoelectrons).

one branch of an hyperbola parametrized as $y = p_1\sqrt{1+(x-x_0)^2/p_0^2}$. The Cherenkov angle can be extracted from the ratio of the two parameters p_0 and p_1, while the (x,y) coordinates of the apex of the hyperbola are given by the x_0 and p_1 parameters, respectively. For two particles with the same momentum, but different mass, at normal incidence on the radiator, the vertical position of the apex is shifted, therefore the reconstruction error on this parameter is related to mass separation. First, a large sample of 30 GeV/n Ar ions were generated by GEANT4 and the Cherenkov light generation and transport along the whole FDIRC prototype was modelled, including the light losses in the insensitive regions between adjacent arrays on the focal plane. For a selected sample of non-interacting Ar ions, each event was fitted to an hyperbola. The distribution of the reconstructed vertical position of the apex of the hyperbola was fitted with a Gaussian with a σ_{MC} $\sim$31 μm to be compared with the 200 μm pitch of the vertical SiPM pixels of the array. The same procedure was repeated using a selected sample of non-interacting Ar ions from the beam test data at the same energy (Fig. 2d). The experimental value for σ_{data} $\sim$63 μm is in reasonable agreement within a factor 2 with the the MonteCarlo.

6. Conclusions

The beam test data confirmed the expected performance of the FDIRC prototype in achieving elemental charge separation of the beam fragments with an integral measurement of the Cherenkov light. The SiPM arrays provided single photon sensitivity, stable operations and a clean measurement of the number of photons collected on the focal plane, allowing to operate the instrument as a digital device in photon counting mode. Extrapolation of the MC simulations to a detector with a larger aperture (mirror lateral size) and focal plane coverage is under way.

References

[1] I. Adam et al., Nucl. Instrum. Meth. A 538 (2005) 281
[2] T. Kamae et al. BELLE Note 49, January 1995
[3] B.N. Ratcliff, Nucl. Instrum. Meth. A 502 (2003) 211
[4] T. Kamae et al., Nucl. Instrum. Meth. A 382 (1996) 430
[5] K. Föhl et al., Nucl. Instrum. Meth. A 595 (2008) 88
[6] J. Va′vra, SLAC-PUB-13763 October 27, 2009 (Addendum on December 15, 2009)
[7] P.S. Marrocchesi et al., Astroparticle Physics 35 (2011) 21âĂŞ27
[8] M.E. Wiedenbeck and D.E. Greiner, D. E, Astrophys. J. 239 (1980) 139
[9] E.C. Stone et al., Space Science Reviews 86 (1998) 285
[10] T. Hams et al., ApJ 611 (2004) 892
[11] J. Cohen-Tanugi et al., SLAC-PUB-9735, 2003
[12] F. Acerbi, et al. IEEE Transactions on Nuclear Science, Volume:62, Issue:3 (2015)
[13] C. Piemonte, et al. Proc. IEEE-NSS/MIC Conference-Seoul (2013) M14-2
[14] M. Y. Kim, et al. Nucl. Instrum. Meth. A, vol. 703 (2013), 177-182
[15] P.S. Marrocchesi, et al. Nucl. Instrum. Meth. A, vol. 659 (2011) 477–483
[16] P.S. Marrocchesi et al., IEEE Transactions on Nuclear Science, Vol 61 (2014) 2786-2793